Science of the Total Environment 954 (2024) 176730

Contents lists available at ScienceDirect

Science of the Total Environment

journal homepage: www.elsevier.com/locate/scitotenv

Predicting the impact of underwater skimming on dissolved oxygen consumption in slow sand filters for potable water treatment

Tolulope Elemo [a], Michael Chipps [b], Nigel Graham [c], Andrew Turner [d], Bruce Jefferson [a], Francis Hassard [a,*]

[a] Cranfield University, Cranfield MK43 0AL, UK
[b] Thames Water Utilities Limited, Kempton Park AWTW, Hanworth TW13 6XH, UK
[c] Imperial College London, Department of Civil and Environmental Engineering, London SW7 2AZ, UK
[d] Essex and Suffolk Water, Chelmsford CM3 8BD, UK

HIGHLIGHTS

- Hydraulic loading rate key to DO recovery post-cleaning pause.
- Pause duration between 3 and 24 h less critical for DO recovery.
- Model predicts DO within ±0.6 mg/L, validating its utility for DO management in SSF.
- UWS with sweetening flow enhances DO replenishment.
- UWS reduces downtime due to cleaning, improving potential water production volume in SSF.

GRAPHICAL ABSTRACT

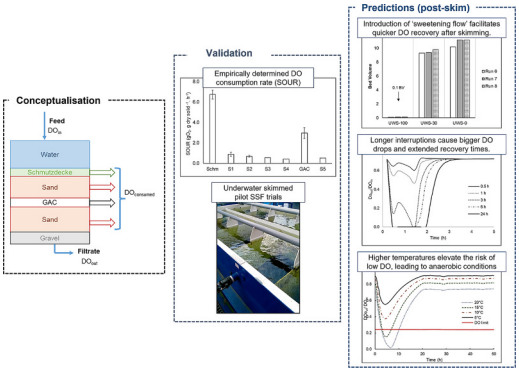

ARTICLE INFO

Editor: Jan Vymazal

Keywords:
Dissolved oxygen
Slow sand filter (SSF)
Underwater skimming (UWS)
Schmutzdecke

ABSTRACT

In a well-functioning slow sand filter (SSF), dissolved oxygen (DO) is crucial for enabling aerobic processes and microbiota growth. Given that DO supply is predominantly via the feed water, flow pauses (e.g., during cleaning) may trigger anoxic/anaerobic conditions in the stagnant filter bed. Underwater skimming (UWS) is an advanced cleaning technique that employs a skimmer with a shrouded blade, mounted on a mobile platform, to remove the fouling layer composed of sand and particles in order to improve the efficiency of slow sand filtration. As UWS results in changes to the flow pattern of the SSF, a mathematical model was developed to predict DO utilization after a flow perturbation associated with UWS operation. The model was based on a depth resolved measurement of specific oxygen utilization derived from a full scale SSF. Pilot plant experiments monitored DO in the feed and filtrate of SSFs cleaned using underwater and conventional dry skimming techniques. The highest oxygen utilization was in the *Schmutzdecke* layer, with additional demand imposed by the presence of a granular activated carbon (GAC) sandwich layer. It was observed that pseudo-steady state conditions occurred following filter ripening, where DO utilization, driven by biological activity, remained relatively constant regardless of filter cleaning technique. For flow pauses between three and 24 h, the pause duration's importance decreased, while

* Corresponding author.
E-mail address: francis.hassard@cranfield.ac.uk (F. Hassard).

https://doi.org/10.1016/j.scitotenv.2024.176730
Received 8 August 2024; Received in revised form 30 September 2024; Accepted 2 October 2024
Available online 10 October 2024
0048-9697/© 2024 The Authors. Published by Elsevier B.V. This is an open access article under the CC BY license (http://creativecommons.org/licenses/by/4.0/).

the hydraulic loading rate became the critical factor for DO recovery in the filter. Additionally, introducing a 'sweetening flow' during UWS ensured a continuous DO supply, facilitating quicker DO replenishment post-cleaning. The model reliably predicted filtrate DO within ±0.6 mg/L, demonstrating its operational utility, especially in the optimisation of UWS methodology. As such, UWS can be applied to clean SSFs with the methodology modified to prevent any detrimental effects to DO management within the filter. This study predicted DO dynamics in SSFs, advancing UWS techniques and could be applied for enhancing water treatment strategies by filtration.

1. Introduction

Slow sand filtration is an effective, robust and simple treatment process that requires minimal energy and chemical input, with contaminant removal occurring through both physical and biological mechanisms (Maiyo et al., 2023). Slow sand filters (SSFs) are predominantly positioned after primary roughing filtration, or other pre-treatment processes such as ozonation to improve treatment (Abdiyev et al., 2023). In certain instances, such as within the Dutch water sector, SSFs are utilized as a concluding treatment step to enhance the biostability of drinking water (van der Kooij et al., 2017). In all cases, it is believed that the critical functional component of a SSF is the *Schmutzdecke*, a microbial biofilm layer formed by turbidity-causing materials, biodegradable organic matter, and algae on, and within, the sand bed surface. Consequently, the contaminant removal capacity is principally concentrated in the top layers (<50 mm) of the SSF bed where there is heightened activity (Trikannad et al., 2023).

The biological processes within a SSF predominantly function in an aerobic environment and hence ensuring sufficient DO within the bed is crucial. Temperature and seasonal shifts can modulate DO utilization, with warmer waters leading to intensification of microbial metabolism and organic matter decomposition (Steele et al., 2006). The primary DO source is the feed water, with a supplementary contribution diurnally from daylight photosynthesis by algae (Ellis, 1985). Furthermore, perturbations in filtration rates or flow can hinder the continuous DO supply, inducing anaerobic or anoxic conditions leading to a reduced treatment and a decline in grazer organisms and consequently, pathogen removal (Elliott et al., 2011).

Headloss resulting from the accumulation of particles, algae, and biofilm growth necessitates regular cleaning to ensure the system operates at its intended flow rate. This maintenance usually entails removing the top layer of sand, which is typically between 10 and 50 mm deep using mechanized techniques including robotic dry skimming devices (Cullen and Letterman, 1985). Conventional cleaning methods like dry skimming require the filter to be drained before cleaning, resulting in substantial operational downtime accounting for up to 90 % of the total downtime associated with SSFs (1–3 days). The removed sand is then cleaned, ready for reuse.

An alternative technique, underwater skimming (UWS), has been introduced to address this inefficiency by cleaning the bed while still submerged, of which a number of variants exist including a shielded blade, a vacuum system, or a floating dredging device (Hassard et al., 2022). In such cases, microbial oxygen utilization persists and within the beds the DO can reduce below an agreed operational limit of 3 mg/L heightened risk of anaerobic or anoxic conditions within the bed (Burman, 1978). This has previously been reported in intermittently operated SSFs where anoxic zones have formed during periods of minimal flow or submersion lasting 24 h or more (Young-Rojanschi and Madramootoo, 2014).

Many SSFs employ an in-bed layer of GAC (~10 cm) to assist in micropollutant elimination, a process that amplifies the demand for DO due to both abiotic sorption and biotic consumption (Steele et al., 2006). The GAC layer is seldom replaced (for example >70,000 bed volumes or 3–30 years' operation), thereby encouraging microbial growth and biodegradation as the primary pollutant removal mechanism (Velten et al., 2011). As such, in an acclimated GAC layer, DO utilization may be largely attributed to biological activities (Eighmy et al., 1993). The overall DO utilization within SSFs raises concerns around the risk associated with underwater skimming leading to periods of operation below the 3 mg/L DO set point. To date, there is a paucity of information concerning declining DO patterns and no model currently exists to effectively predict DO as a function of operational parameters.

Accordingly, the aim of this study was to investigate the impact of UWS operation on the risk of depleting the DO below the operational limit during periods of flow pause. The research aimed to elucidate how variables such as filter media depth, stagnation durations, water temperature, feed DO concentrations and 'sweetening flow' during skimming might affect SSF performance during these periods. 'Sweetening flow' in this study refers to the flow through a SSF (i.e., a percentage of the normal operational flowrate) while skimming underwater. To achieve this, specific oxygen consumption data collected from a full-scale SSF were used to develop a model of DO utilization. This model was subsequently tested and validated through a series of pilot-scale filtration experiments conducted with real water from an operational treatment works, involving four different filter runs and three skimming events, thereby enabling direct observation of DO utilization in pilot SSFs.

2. Materials and methods

2.1. Pilot filtration setup

Pilot experiments were carried out at the Thames Water Research, Development and Innovation Centre, located in Kempton Park AWTW, Hanworth, UK, from March 2021 to June 2022. The pilot plant encompassed ten identical, individual filters, each with a surface area of approximately 0.54 m^2. The composition of each filter bed included a layer of sand (0.2–0.5 m in depth, effective size = 0.3 mm, uniformity coefficient = 1.8), a layer of GAC (0.1 m in depth, effective size = 0.6 mm, uniformity coefficient = 1.9), followed by a 0.2 m fixed sand layer, and a 0.1 m gravel support layer stacked vertically above each other in the order top to bottom (Fig. 1). The pilot plant received its feed water from a storage reservoir directly connected to the river Thames (a surface water source) and had an approximate retention time of 30 days. The operational flow rate was a target value of 0.3 m/h, which required regular- checking and was adjusted as headloss developed. Over the 15-month operational trial, the DO concentration of the feed water averaged 10.5 ± 2.3 mg/L, total organic carbon (TOC) was 3.6 ± 0.2 mg/L, turbidity was 0.6 ± 0.4 NTU, and pH was 8.1 ± 0.2. Filters were operated at ambient air temperature (−6 to 22 °C) with water temperature ranging from 3 to 16 °C.

All filters underwent similar operation procedures except for the cleaning methodology, which served as the primary distinguishing factor and was replicated on 2 filters. DO measurement was only made on one of each replicate. Cleaning methodologies implemented encompassed UWS and varying flow percentages (0, 30 and 100 % of full flow rate, i.e., 0 m/h, 0.09 m/h and 0.3 m/h) and traditional dry skimming, which served as the control (Table 1). Dry skimming was carried out with a custom-made scraper and shovel (both disinfected with 70 % ethanol between uses). UWS was performed using a commercial wet/dry vacuum cleaner (Kärcher WD 5/P, 1100 W, 240 V) modified with a custom-designed scraper attachment. The scraper was fabricated from

stainless steel, measuring 300 mm in width and 50 mm in height, with an adjustable shroud to control the depth of sand removal. The vacuum hose was connected to the scraper, allowing simultaneous suction of sand and water during skimming while the filter remained submerged. The power of the vacuum cleaner was sufficient to remove the top 10–50 mm layer of sand effectively without disturbing the underlying layers.

UWS was conducted at different sweetening flow percentages of the operational hydraulic loading rate (HLR) — 100 %, 30 %, and 0 % (Table 1). Post-skimming, filters were adjusted to the operational HLR using the 24-h 0.1 m/h increment method. For instance, the UWS-100 did not necessitate any increments as skimming was executed at operational HLR, whereas both UWS-30 and UWS-0 required two increments each.

DO was measured via luminescence probes (Hach, Loveland, Colorado, USA) calibrated weekly using manufacturer's instructions and sampled every 15 min. The filters were scraped after operational setpoints of headloss, or time were reached, which ever limit was reached first. The longest time for operation was 70 days, which aligns with the local water utility operational guideline. While in most cases headloss was the operational trigger to clean the SSF, the exception was after filter 'resand' events when time was the factor as the headloss did not meet the setpoint after 70 days. Three individual filter runs were captured for this DO study, with run lengths of 71, 41 and 43 days for runs I, II and III respectively. Detailed DO levels in the feed and filtrate of 5 beds were captured for these runs and 4 beds reported here. Each filter run was split into *pseudo*-steady state operation (i.e., 14 days into the filter run, as further described in Section 2.3) and dynamic state operation (i.e., during skimming and flow pause). A total of nine unique data sets were recorded during dynamic states (3 each for UWS-100, UWS-30, and UWS-0 for the 3 filter runs).

2.2. Specific oxygen uptake rate (SOUR) of biologically active media

The SOUR for the SSF media at various depths, which encompassed the biofilm in both the sand and GAC layers, was assessed by modifying the method outlined in Method 1683 (US EPA, 2001). The samples used for the SOUR measurement were taken from a full-scale SSF bed with a surface area of 3082 m^2. This bed had been operational for 56 days since its last conventional dry skim. The total volume of water treated by the GAC within this SSF was roughly 68,000 bed volumes. The full-scale SSF was selected for sampling because it offered a more accurate representation of the microbial state of an actively functioning process. The sampling process was conducted at the conclusion of an operational cycle, with three randomly chosen locations. At each of these sites, a hole measuring 0.25 m by 0.25 m was created, from which horizontal core samples were extracted at varying depths.

Table 1
Description of the different skimming treatments performed in the SSF pilot facility, with corresponding measured rates of DO consumption.

Skimming (UWS[1]/dry)	Sweetening flow[2]	Total time left dry (h)[3]	ID[4]
UWS	100 %	0	UWS-100
UWS	30 %	0	UWS-30
UWS	0 %	0	UWS-0
Dry	n/a	14	DS

[1] UWS refers to Underwater skimmed beds.
[2] Sweetening flow is the percentage of the operational filtration rate (0.3 m/h) allowed during skimming.
[3] Total time left dry is the duration where a filter was left completely dry before, during and after skimming.
[4] ID is the identity of each treatment in the graphs and discussions.

The depth ranges sampled were: 0–25 mm (Sch), 25–50 mm (S1), 50–100 mm (S2), 100–200 mm (S3), 100 mm above GAC (S4), within the GAC (GAC), and below the GAC layer (S5). The three samples collected from the different locations were carefully combined to form a composite sample for each depth. Each composite sample was placed into a 300 mL flask, previously cleaned with a 10 % HCl solution and heat sterilised at 150 °C. Each flask, containing a magnetic stirrer, was then filled to achieve a total solid concentration of 20 g/L using sterile 0.01 M phosphate-buffered saline (PBS) solution with a pH of 7.4. DO probes (Hach LDO101, using Luminescent method) were used to measure DO readings over a 15-min period. The measurements were taken at 15-s intervals for the first 2 min and 1-min intervals for the remainder of the experiment. Prior to the experiment, DO probes were calibrated according to manufacturer instructions. Temperature control throughout the process was maintained at ±0.2 °C using a heated water bath. Lastly, the volatile solid (VS) content of the media/biomass was measured according to Method 1684 (US EPA, 2001). The SOUR was calculated as:

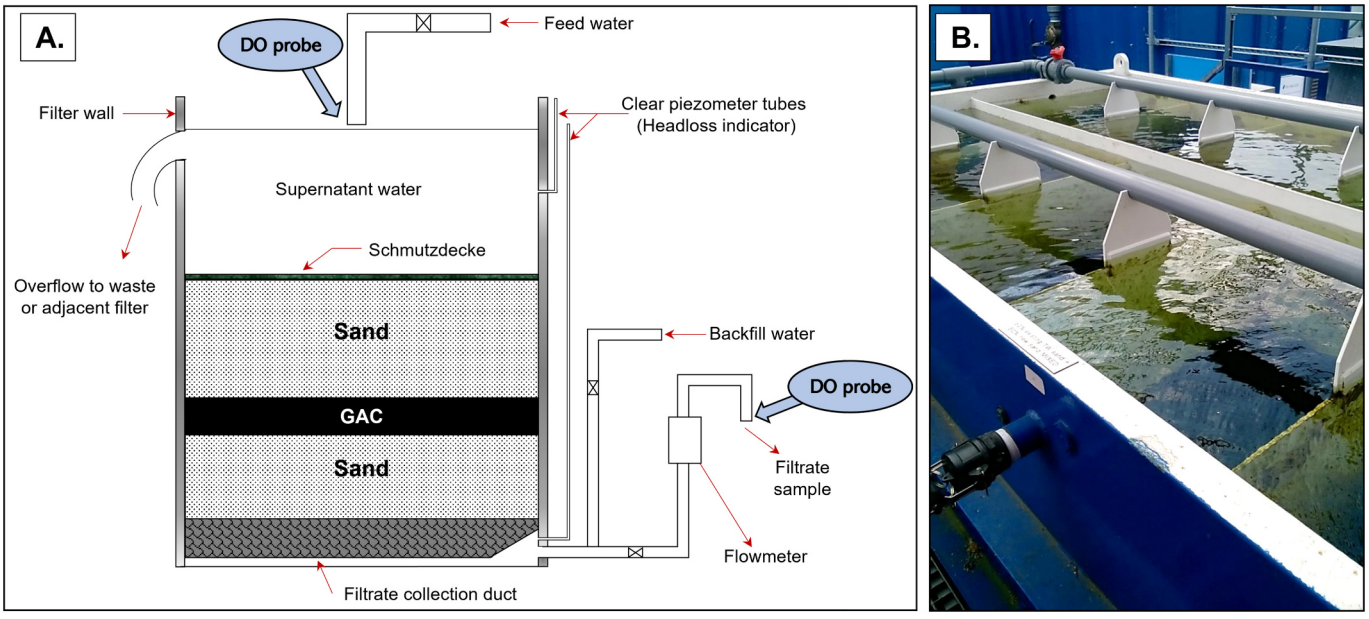

Fig. 1. (A) Schematic illustrating a cross-sectional representation of each test filter incorporated within the pilot SSF facility to demonstrate the layout and configuration. (B) Photographic image displaying the 10 individual cells of the pilot SSF facility, illustrating its physical structure and design.

$$SOUR_T = \frac{OUR}{TS} \times \frac{60\ min}{\text{h}} \times \frac{1}{VS} \quad (1)$$

where:$SOUR_T$ = specific oxygen uptake rate in the sample at analysis temperature, T (mg O_2/g VS)/hOUR = oxygen uptake rate in the sample (mgO_2/L)/min. This is the slope of a plot of observed readings (DO, mg/L) versus time (min)TS = total solids in the analysis sample (g/L)T = temperature of the sample during analysis, °CVS = volatile solids of media aliquot (g VS/g).

Values were corrected for temperature using:

$$SOUR_{20} = SOUR_T \times \theta^{(20-T)} \quad (2)$$

where:$SOUR_{20}$ = specific oxygen uptake rate at 20 °C (mgO_2/gVS)/hθ = temperature correction factor, 1.05 above 20 °C, 1.07 below 20 °C.

2.3. Modelling DO utilization

A mass balance model was developed to study the potential impact of UWS operations on the profile of DO in a SSF. The SSF bed was modelled as an assembly of layers comprised of the *Schmutzdecke* layer (defined as the top 25 mm), sand layers, and GAC layers, where the numerical algorithm contains layers between which there are flows (Fig. 2). The gravel support layer was excluded from the model since our empirical data suggested negligible oxygen consumption in this layer (see Supplementary information).

The amount of DO utilization was estimated using a mass balance approach, under the following assumptions:

1. Negligible mass transfer from the gas phase to the bulk liquid.
2. DO adsorption onto media grains (sand and GAC) was deemed negligible compared to biological utilization.
3. The biofilm was homogeneous on individual media grains or within layers in terms of both its mass and activity.

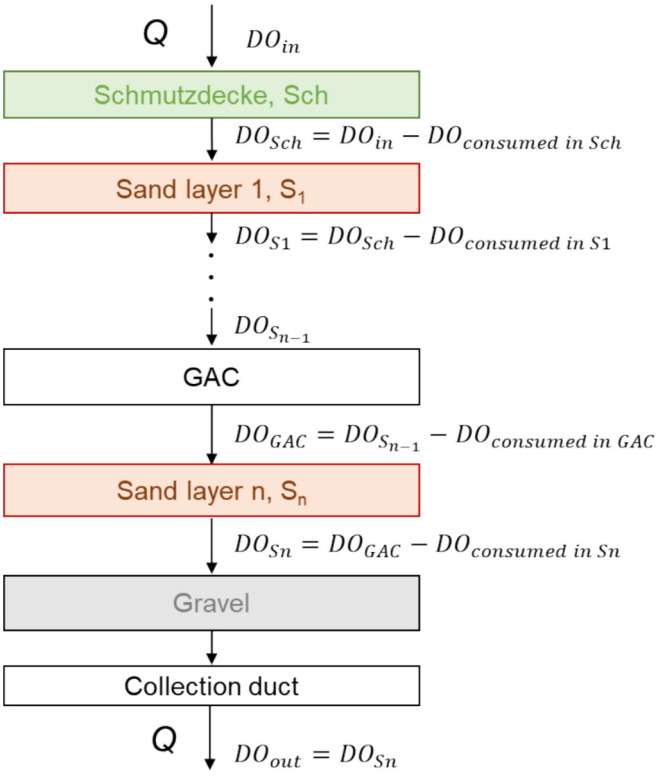

Fig. 2. Conceptual representation of the mathematical model in terms of the flow of DO through a biologically mature SSF that features a GAC layer.

4. Excluding the *Schmutzdecke*, the biofilm is considered to be in a pseudo-steady state, implying that the biofilm mass and activity remain relatively constant over time.
5. The activity within the *Schmutzdecke* maintains a steady state, even though the mass of the *Schmutzdecke* continues to grow.
6. The generation of DO within the filter can be considered as negligible, and any accumulation was also assumed to be zero.

2.3.1. Pseudo steady state operation

At steady state, the general mass balance equation can be presented as follows:

$$\frac{dC(x)}{dx} = -\frac{k(x)C(x)}{Q} \quad (3)$$

where:

- C(x) is the DO concentration at depth x,
- k(x) C(x) represents the rate of DO consumption per unit volume, consistent units of mass per time.

A SSF is considered to be in a steady state once the *Schmutzdecke* layer is fully developed — a stage referred to as a 'ripened SSF'. A SSF is considered to reach a steady state once the Schmutzdecke layer is fully developed, a stage referred to as a 'ripened SSF'. In the context of this study, this state was assumed to occur after 14 days of continuous operation, based on consistent observations of *Escherichia coli* removal efficiency and filtrate turbidity stabilization obtained from both pilot and full-scale studies conducted by the local water utility. The consumption of DO is a function of the SOUR within individual layers. Thus, the DO consumption in each individual layer can be expressed as follows:

$$r_i = SOUR_i \times VS_i \times \tau_i \quad (4)$$

where r_i is the DO consumption within an individual layer, i (mg. (g dry solid)$^{-1}$), and τ_i is the residence time within the individual layer (h), calculated as:

$$\tau_i = \frac{V_i}{Q} \quad (5)$$

where V_i is the volume of individual layer (L) and Q is the operational flowrate (L/h). The mass of DO consumed in each layer, M_i (mg) is thus a product of the consumption and the mass of media in the layer, w_i (g).

$$M_i = r_i \times w_i \quad (6)$$

The modified mass balance for DO in the filter can be re-written as:

$$DO_{out} = DO_{in} - \sum_{i=1}^{N} r_i.w_i \quad (7)$$

In this equation, N represents the total number of layers. For the sand layers above the GAC, the value of N decreases with each filter run due to the removal of the *Schmutzdecke* and underlying sand layer.

2.3.2. DO utilization under dynamic conditions: skimming and flow pauses

The UWS occurs when the filter is completely submerged in water, with a continuous flow (of some proportion of normal flow). However, in a situation where there is no flow — meaning there is no incoming or outgoing water — the individual layers in the filter behave similarly to a batch reactor in terms of DO consumption. At the starting point ($t = 0$), a definite volume of water is present within each layer, providing a mass of DO, denoted as m_i (mg). During flow pauses when Q = 0, the model treats each layer as a batch reactor. The DO concentration in each layer depletes over time due to microbial consumption

$$m_{i,0} = DO_{i,0} \times V_i \bullet \varepsilon_i \quad (8)$$

where ε_i is the effective porosity of the media (dimensionless).

The amount of DO within each distinct layer is progressively depleted during the pause in flow. Following the removal of the *Schmutzdecke* layer, the rate of DO consumption within the remaining layers is hypothesized to remain consistent with the rate observed just prior to the pause. Consequently, the amount of DO consumed during this period of paused flow can be represented as:

$$R_i = (r_i \cdot w_i) \times t \quad (9)$$

where t is the duration for which the flow was paused (h).

The mass of DO left in the filter at the end of the pause (and the start of a new filter run) is:

$$m_{i,t} = m_{i,0} - R_i \quad (10)$$

The DO concentration in the individual layers is thus:

$$DO_{i,t} = \frac{M_{i,t}}{V_i} \quad (11)$$

Upon re-establishing flow, the filter takes on characteristics akin to a plug flow reactor. This implies that there is no interlayer mixing, but perfect intralayer mixing. The consideration is applied to the volume of water within each layer separately. The DO input for each successive layer is the reduced DO content from the preceding layer, for instance $DO_{i+1,t} = DO_{i,t}$.

In the majority of SSFs, a collection duct at the bottom of the filter exists. It is assumed that there is no further DO consumption within this collection duct, and complete mixing occurs, leading to a consistent DO concentration at any given moment. When the flow is interrupted, $DO_{duct} = DO_{N,t}$. Once flow is resumed, the DO in the duct becomes:

$$DO_{out} = DO_{duct} = DO_{N,t} - \frac{V_{N,t+x}}{V_{duct}}\left(DO_{N,t} - DO_{N,t+x}\right) \quad (12)$$

where $V_{N,t+x}$ is the volume treated in the time x after flow is resumed.

During periods of 'sweetening flow' the filtration rate is partially reduced and a continuous movement of water persists through the filter which results in a consistent DO supply. As a result, the filter operates similarly to a plug flow reactor, with DO consumption happening as the water navigates through the distinct layers. The model parameters used in the simulations are summarized in Table 2.

2.3.3. Model validation, sensitivity and limitations

To evaluate the accuracy of the developed model in predicting DO consumption, the root mean square error (RMSE) was computed, comparing the predicted and observed DO concentrations in the filtrate. For the validation of the model, the deviations were found to be minimal, with a RMSE value of 0.6 mg/L based on 45,170 data points collected from five pilot SSFs over three filter runs. Additionally, the dataset underwent Bland-Altman analysis — a statistical method employed to assess agreement between two quantitative measurements. A Bland-Altman plot juxtaposes two measurements by plotting the difference against the average. The average difference reflects the estimated bias, while the standard deviation accounts for random variations. If differences within the mean ± 1.96 SD (which represents 95 % of data in a normal distribution) are deemed insignificant, the methods can be interchangeably used. These boundaries signify the limits of agreement (Altman and Bland, 1983; Bland and Altman, 1999).

A sensitivity analysis was performed to assess the model's responsiveness to changes in operational conditions and skimming scenarios, including variations in submersion durations, flow re-introduction regimes, and temperature fluctuations. This aimed to predict DO consumption post-skimming in a SSF using the UWS-0 method.

In every scenario studied, filtrate DO levels consistently remained above 0 mg/L, with no anoxic or anaerobic conditions observed. This study did not explore how such conditions might affect the SOUR and subsequent oxygen usage. Nitrate monitoring during pilot experiments, however, indicated no usage of alternative electron acceptors, evidenced by the absence of net nitrate removal.

Table 2
Model parameters.

Description	Symbol	Unit
Depth of GAC layer	L_{GAC}	m
Depth of sand layer 1	L_{S1}	m
Depth of sand layer 2	L_{S2}	m
Depth of sand layer 3	L_{S3}	m
Depth of sand layer 4	L_{S4}	m
Depth of sand layer 5	L_{S5}	m
Depth of *Schmutzdecke* layer	L_{sch}	m
Dissolved oxygen concentration	DO	mg/L
Dissolved oxygen consumption within individual layers	r_i	$mg \cdot g^{-1}$
Effective porosity of media	ϵ_i	Dimensionless
Flow pause duration	t	h
Flowrate	Q	L/h
Hydraulic loading rate	HLR	$m \cdot h^{-1}$
Mass of dissolved oxygen consumed within individual layer	M_i	mg
Mass of dissolved oxygen within layers during flow pause	m_i	mg
Mass of DO consumed during pause	r_i	mg
Mass of media in individual layer	w_i	g
Residence time within individual layers	τ_i	h
Specific oxygen uptake rate	SOUR	$mg \cdot h^{-1} \cdot gVS^{-1}$
Temperature correction factor	θ	Dimensionless
Total depth of filter bed	L	m
Volatile solid	VS	$gVS.g^{-1}$
Volume of collection duct	V_{duct}	L
Volume of individual layers	V_i	L

Details of the filter runs used in model

Filter run	Run length (days)	Media depth (m)
I	71	0.80
II	41	0.76
III	43	0.72

3. Results

3.1. DO utilization with filter depth

The *Schmutzdecke* layer exhibited the highest oxygen utilization rate per unit mass of media at 6.74 ± 0.44 g O_2·g dry $solids^{-1}$ h^{-1} (Fig. 3). The oxygen utilization rate consistently diminished with depth down to a rate of 0.43 ± 0.01 g O_2·g dry $solids^{-1}$ h^{-1} for S4 until the GAC layer, where it increased by over fivefold compared to the sub-sand layers to a rate of 0.52 ± 0.01 g O_2·g dry $solids^{-1}$ h^{-1}. This finding is consistent with previous observations, such as those by Steele et al. (2006), where it was found that DO drop was greatest within the GAC sandwich layer (between 6 and 12 mg/L) compared to the sub-sand layers (between 0.5 and 2.5 mg/L). The enhanced demand in the GAC layer can be linked to the large surface area it provides to support microbial growth (Wang et al., 1995). Though SOUR is not a direct measure of biological activity, it serves as a valuable indicator for assessing biological degradation (van der Aa et al., 2011).

3.2. DO utilization under steady state and dynamic operation

Throughout the pseudo-steady state periods of the trials, the DO consumption (difference between feed and filtrate DO) was between 2.0 and 5.0 mg/L. This occurred as the DO increased in both the feed and effluent (Fig. 4). To illustrate, in the case of a UWS operated with a 100 % sweetening flow, the DO of the feed increased from 8.3 to 12.3 mg/L over the 60 days of the run with the effluent DO changing from 4.2 to

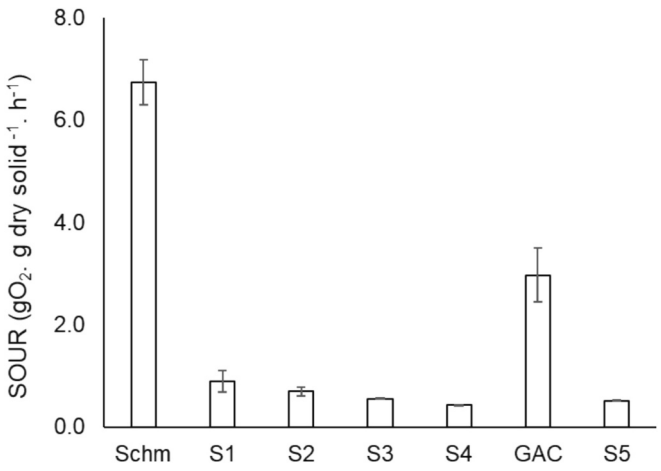

Fig. 3. Profile of SOUR with bed depth: *Schmutzdecke* (Schm); S1: 25–50 mm; S2: 50–100 mm; S3: 100–200 mm; S4: 200 – top of GAC layer; GAC: GAC layer; S5: below GAC layer. Composite samples collected from 3 different spatial locations within a mature SSF. Error bar represents average ± standard deviation (n = 3). SOUR values were corrected to 20 °C using Arrhenius equation to describe temperate dependency.

8.7 mg/L over the same time period. Importantly this trend persisted for all monitored filters, indicating that the different skimming arrangements did not influence biological activity. Throughout the period of operation, the DO level in the filtrate did not go below an operational minimum of 3.0 mg/L DO and hence revealing that UWS poses minimal risk in terms of maintaining suitable DO levels.

Under dynamic conditions (defined in this study as during and immediately after skimming), particularly during UWS without a sweetening flow (UWS-0), the rate of oxygen consumption during skimming was consistent at 2.7 mg O_2/kg media/h, with less than a 5 % difference between the skimming treatments (2.6–2.7 mg O_2/kg media/h) and with good reproducibility between runs I and III (Fig. 5A–I).

When the flow was interrupted as part of the skimming cycle (i.e., either reduced or stopped), the DO present within the water in the filter was consumed while skimming took place. To illustrate, the effluent DO reached a minimum level of 2.7, 1.4 and 1.7 mg/L for runs I, II and III for the scenario with no flow during skimming. Partial flow during skimming ameliorated the decrease leading to a minimum DO in the effluent of 5.6, 6.0 and 3.8 mg/L for runs I, II and III with a 30 % flow (Fig. 5). This shows a benefit of UWS 30 over UWS 0 in avoiding falling below the 3 mg/L DO threshold.

When the flow was resumed, the water with depleted DO levels within the filter bed was replaced with water with greater DO concentration, leading to a return to the pseudo-steady state levels (Fig. 5). The stepwise increase displayed in the figure arises from the SSF operation where the flowrate was progressively increased (by increments of 0.1 m/h). The impact of UWS while maintaining a sweetening flow was demonstrated by the time taken to return to the steady state conditions (Fig. 6). The recovery duration was 0.1 bed volumes (BV) for UWS-100 but extended to between 9.7 and 10.1 bed volumes for UWS-30. This was close to the no flow case of UWS-0 which resulted in recovery times of between 10.1 and 10.9 bed volumes. Consequently, the results indicate that reduced flow sweetening has marginal benefit and that to see the maximum benefit higher sweetening flows will be required.

For the validation of the model, the deviations were found to be minimal, with a root mean square error value of 0.6 mg/L. This suggests a high degree of reliability in the model, with the predicted filtrate DO exhibiting an accuracy of less than ±0.6 mg/L. To further examine the significance of this finding, a Bland-Altman analysis was conducted. In the analysis (Fig. 7), the difference between the observed and estimated filtrate DO was found to lie within ±0.6 mg/L. The results imply a strong agreement between the measured and modelled values and provided confidence pertaining to the model's robustness.

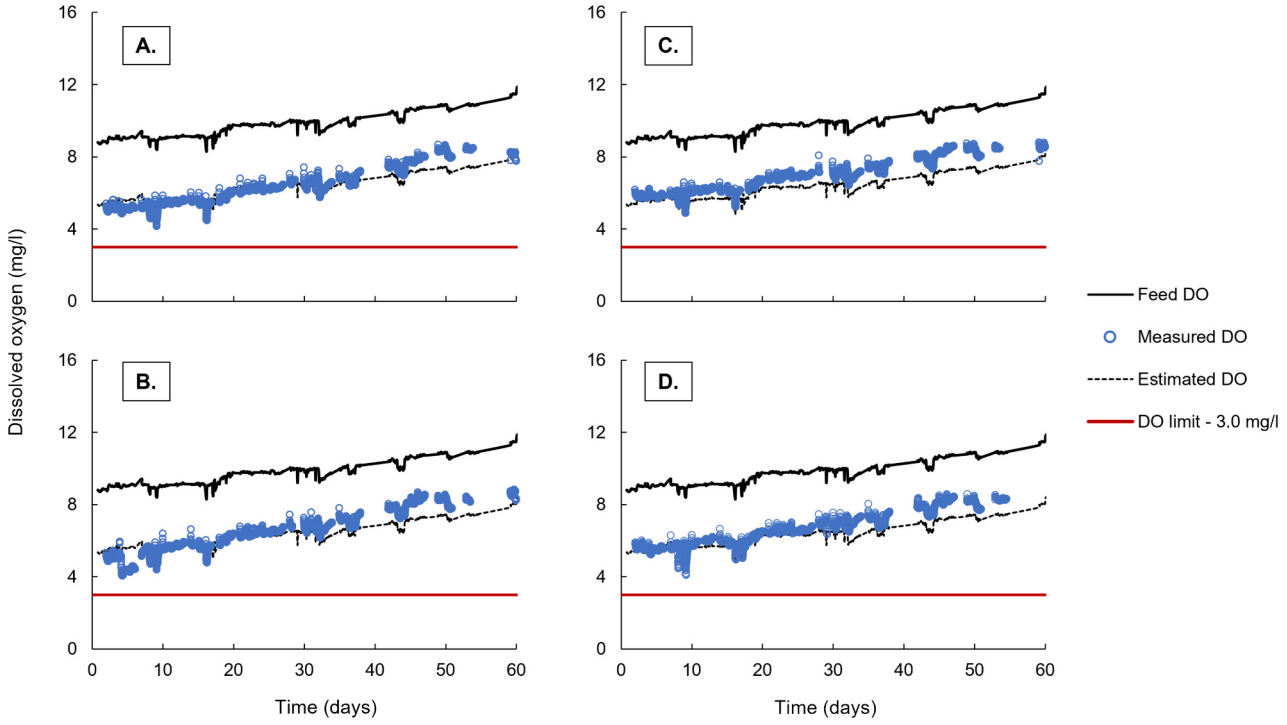

Fig. 4. Observed and model-estimated DO concentrations in the feed and filtrate of the pilot SSFs during one of the filter runs (Run I). The figures show filters that were cleaned using different UWS methodologies: (A) UWS with 100 % operational flow (UWS-100); (B) UWS with 30 % flow (UWS-30); (C) UWS without operational flow (UWS-0); (D) dry skimming (DS) as a control.

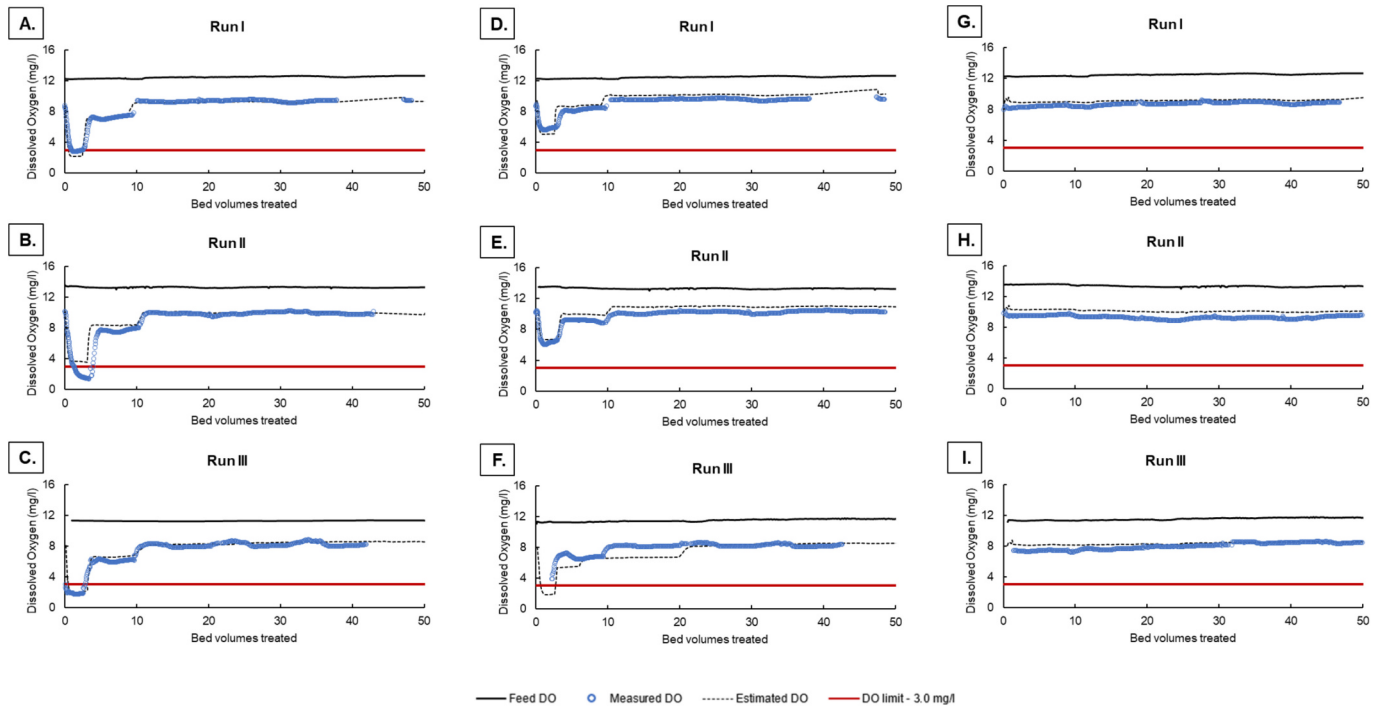

Fig. 5. DO concentrations in the feed and filtrate (observed and estimated from model) in pilot SSFs for different filter runs immediately after skimming: for UWS-0, i.e., skimming done with a flow pause (A–C); UWS-30, i.e., skimming done with reduced flow (D–F); UWS-100, i.e., skimming at operational flowrate (G–I). Hydraulic loading rate increased gradually (in 0.1 m/h increments, up to 0.3 m/h for A–F). Bed volume = 0, is the start of a new filter run. The bed volumes treated is the product of the volumetric flow rate (Q) and time, adjusted for any changes in Q.

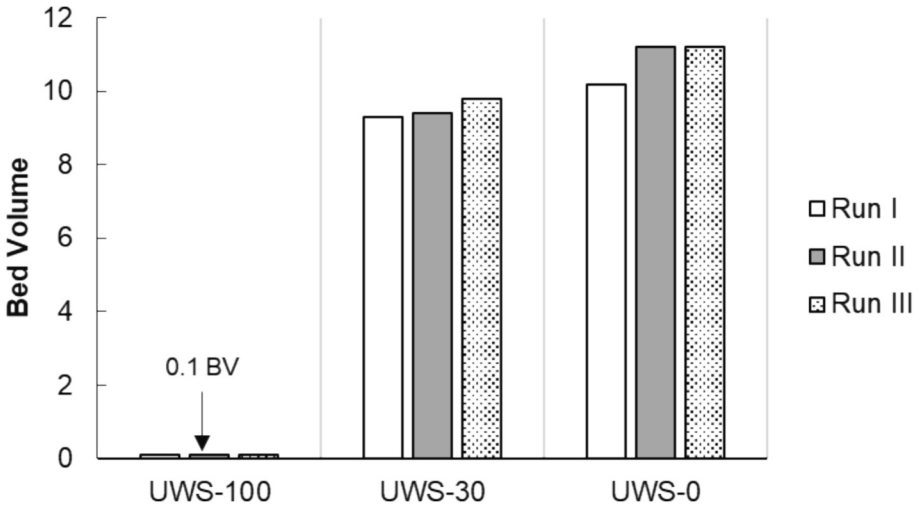

Fig. 6. The impact of sweetening flow on the recovery duration in terms of bed volumes in the pilot SSF post-skimming for Run I (January 2022), Run II (February 2022), and Run III (March 2022).

3.3. Model simulations of how flowrate and its pause duration impact DO utilization

The model was used to investigate the impact of operational variations on the effluent DO and the time to return to steady state conditions (Figs. 8–10). The duration of flow pause significantly influenced both the extent of DO concentration drop within the filter and the recovery time required for the filter to return to pseudo-steady-state conditions. For instance, increasing the pause duration from 30 min to 3 h led to a more pronounced reduction in DO levels of 94 % for a 30 min pause to 99 % after a 3 h pause, and a lengthier recovery period from 2 h to 3 h respectively (Fig. 8). In the scenario of a 24-h flow pause, upon resumption of flow, the DO level fell to below detectable limits (i.e., <0.1 mg/L), denoting complete DO consumption and anoxic conditions within the filter during this extended pause. This happened irrespective of the method of flow resumption (whether incrementally in 0.1 m/h steps or not). However, when the flow was reintroduced swiftly and at a higher rate, the bed's recovery was three times as fast, within only 2 bed volumes required to return to operational DO levels. For the case where the pause exceeds 3 h, the filter risks becoming anoxic. These findings highlight that the HLR post-skimming has a more profound effect on recovery than the flow pause duration during skimming.

When the HLR was reintroduced at a rate of 2.5 %/h, the recovery took about 3.5 times longer (72.3 h) than when it increased by 10 %/h

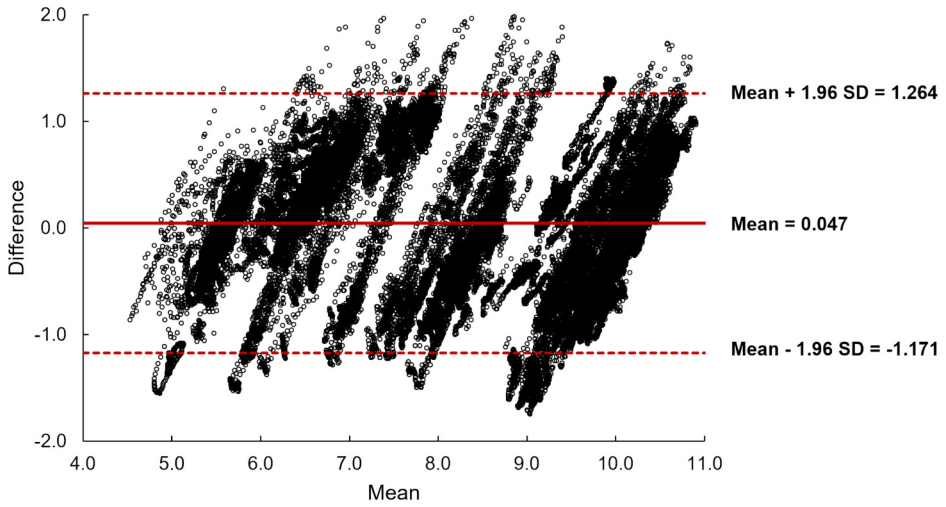

Fig. 7. Bland-Altman plot demonstrating the agreement between observed and estimated filtrate DO under pseudo-steady state conditions. The plot illustrates the difference (observed − estimated) against the mean [(observed + estimated) / 2]. The graph includes results from three distinct filter runs, encompassing a total of 45,170 data points obtained from 5 pilot SSFs.

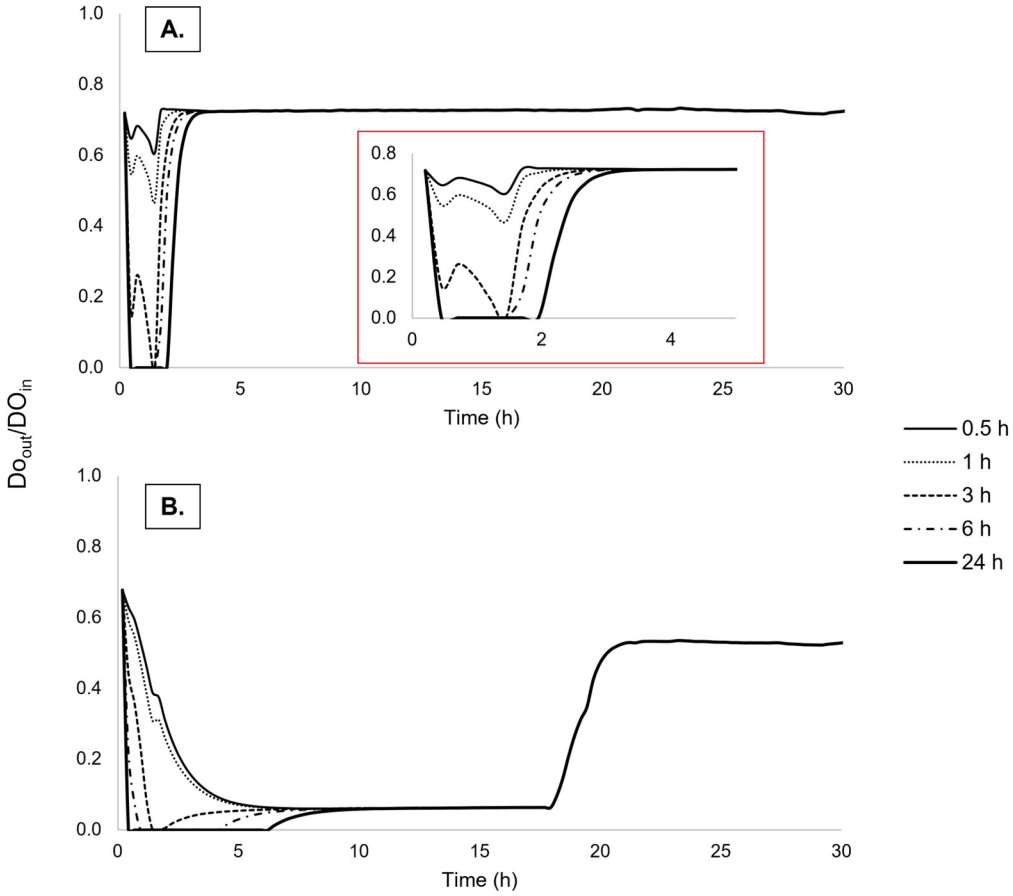

Fig. 8. Impact of pause duration on DO concentrations in the feed and recovery duration subsequent to a flow pause and skimming event (UWS-0). The depicted scenarios were: (A) immediate resumption of flow at full rate post-pause; (B) progressive resumption of flow in stepwise increments post-pause. The conditions assumed a filter bed depth of 0.8 m and an average feed DO concentration of 12.3 mg/L.

(20.7 h). Conversely, an immediate reintroduction of the flow at the operational rate expedited the recovery process, with the filter reverting to a pseudo-steady state DO consumption rate within 2 h of operation. However, operational decisions regarding the flow reintroduction rate post-skimming should consider the limitations of operational systems. For example, it may not be feasible to physically restore the flow to the operational HLR rapidly due to pipe work limitations or site-specific hydraulics. As such, re-introduction flow rates should be increased as quickly as is practically possible, as long other risks from particle penetration which could impact head loss or lead to water quality

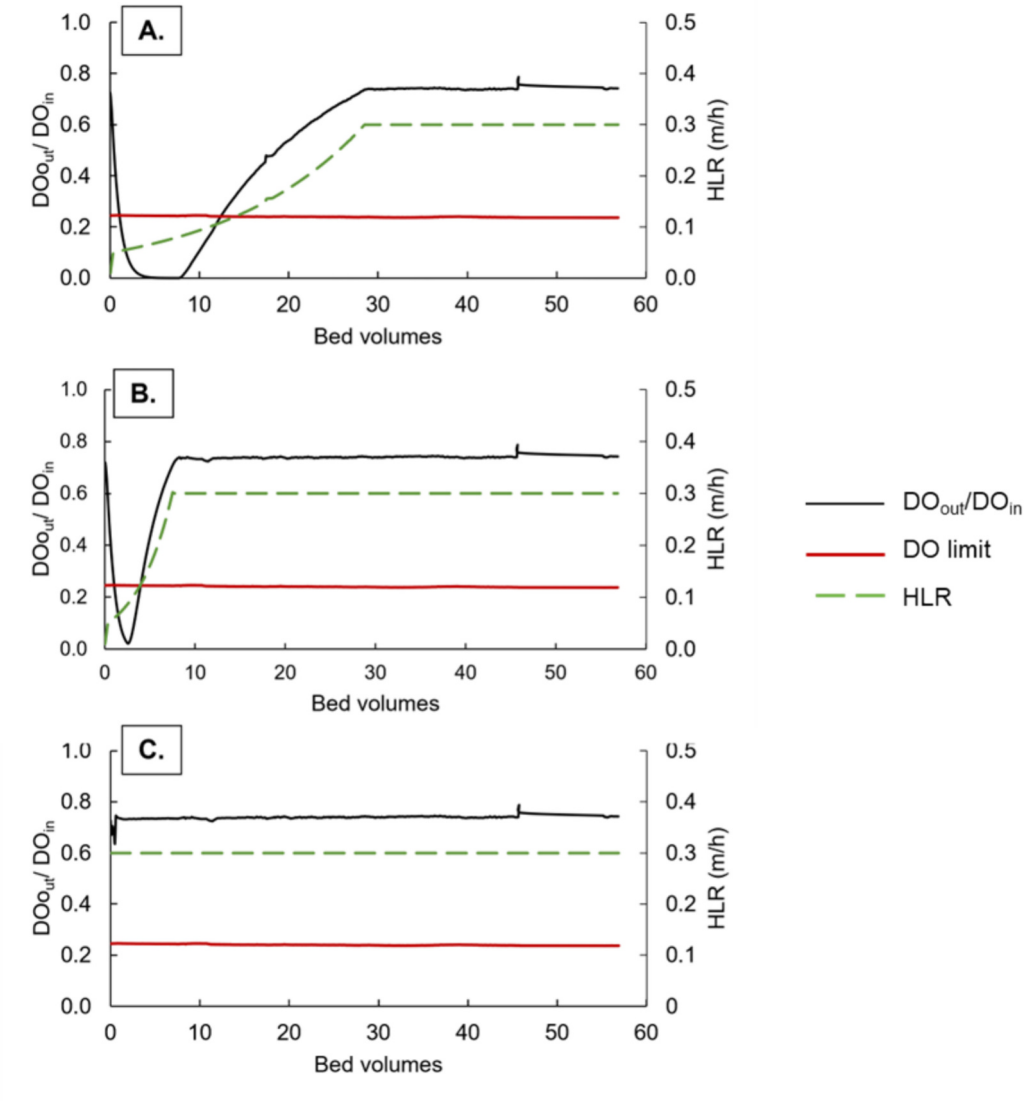

Fig. 9. The predicted influence of HLR on DO supply and consumption in a standard full-scale SSF (with a media depth of 0.8 m, filter surface area of 3082 m^2, and an average feed DO of 12.3 mg/L) immediately post-skimming. Scenarios include: (A) Slow HLR reintroduction at 2.5 % of the operational rate/h; (B) Gradual HLR reintroduction at 10 % of the operational rate/h; (C) Instantaneous return of HLR to the operational rate. Bed volume equals 0 represents the commencement of a new filter run.

concerns.

3.4. The impact of temperature variations on DO utilization in SSF

Predicted forecasts of DO usage at various temperatures when operating a UWS with no sweetening flow showed an increase in DO consumption with rising temperatures from 1.0 mg O_2/kg media/h at 5 °C, to 2.7 mg O_2/kg media/h at 20 °C, for a fixed inlet feed DO concentration of 12.3 mg/L (Fig. 10). The consequence was that at and above temperatures of 15 °C, the DO dropped below the operational limit once flow had been restored. Notably, at 20 °C, the DO concentration was unacceptably low, approaching anaerobic conditions (filtrate DO $<$ 0.3 mg/L), and extended the recovery time to achieve levels above the threshold, taking over 1.5 times longer than at 15 °C. Steady state DO levels were reached after 8 BVs for all temperatures with the actual DO level commensurate with the temperature dependent saturation level. The work shows the combined impact of reduced DO solubility and increased consumption associated with enhanced biological/microbial activities.

4. Discussion

Overall, the findings of this study have shown that UWS can be applied with minimal risk to the biological function of SSFs (Fig. 4). A reduction in filtrate DO can be expected in cases of flow pause or reduced HLR during the cleaning process where consumption out-strips supply. The impact is shown to have a temperature dependency due to the combination of reduced solubility and increased microbial activity as temperatures increase with temperatures above 15 °C requiring specific consideration. Consequently, minimum acceptable sweetening flow rates will either need to be temperature adjusted to ensure DO supply always meets demand or be set at the levels required during the highest temperatures. Importantly, in cases where DO decreased below operational limits (3 mg/L) during the pilot trials, no significant nitrate removal was observed, indicating that the duration of the low DO levels were insufficient for the onset of anoxic/anaerobic activity to develop (Young-Rojanschi and Madramootoo, 2014). In addition, the work has shown the importance of the rate of flow reintroduction post skimming in terms of the recovery time required to return the SSF back to its steady state condition which needs to be delivered at the maximum rate that is

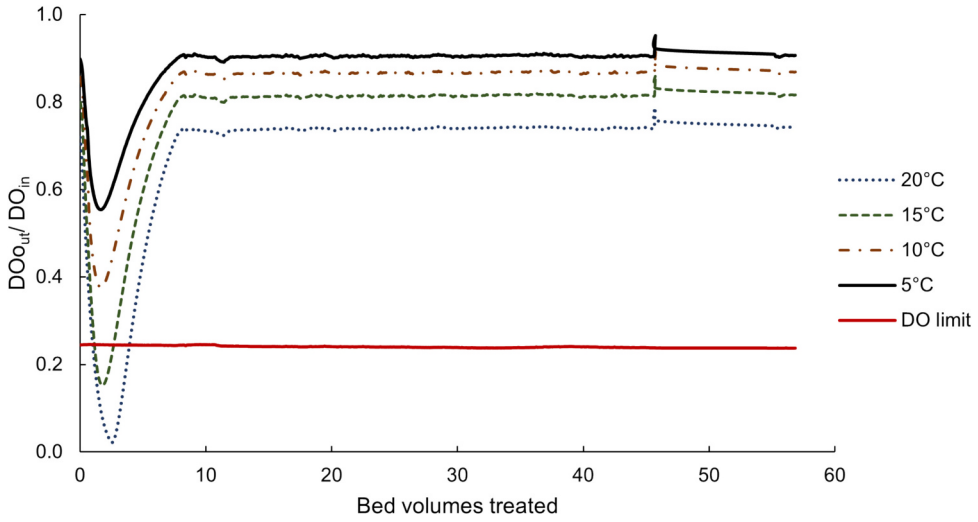

Fig. 10. Illustration of the influence of temperature on the supply and consumption of DO in a full-scale SSF (with media depth of 0.8 m, filter surface area of 3082 m^2, with a GAC layer of 0.1 m, and average feed DO of 12.3 mg/L) post-UWS-0 skimming. The commencement of a new filter run is marked by BV = 0.

practically possible.

Accordingly, the study posits that operational SSFs will have a combination of sweetening flow and the rate of reintroduction that will negate any risk of UWS on maintaining the desired DO conditions within the bed. The current model complements existing SSF models by specifically addressing DO dynamics, which are critical for the biological processes within the filter but have been overlooked in previous models. For instance, models by Schijven et al. (2013) and Langenbach et al. (2010) primarily focus on pathogen removal mechanisms without considering DO consumption. Similarly, headloss and filter run duration models like that of Campos et al. (2006) do not account for the biochemical oxygen demand within the filter bed. Importantly in the context of the current research, none of the models consider the dynamics of DO use during low or no flow operation which represent the case for underwater skimming. Accordingly, our model fills this gap by incorporating empirically derived DO consumption rates at different filter depths, including the impact of temperature and operational variables like sweetening flows. This allows for a more comprehensive understanding of the filter's performance under various conditions, enhancing the ability to predict and manage risks associated with anoxic conditions. By integrating our DO dynamics model with existing models, operators can perform a more holistic assessment of SSF performance, optimizing both microbial safety and operational efficiency. Once validated to a specific site, the model provides a predictive capability to establish the combination of conditions needed. The current model complements existing SSF models and fills an important gap not currently covered by those models. For instance, this model integrates with models designed for pathogen removal (like those suggested by Schijven et al., 2013 and Langenbach et al., 2010), and for forecasting headloss and filter run durations (such as the one presented by Campos et al., 2006). This integration would assist in microbial risk assessment, operational planning and resource management for SSFs across various operating conditions and across multiple filter cycles. The development and validation of our DO dynamics model significantly advance UWS techniques by providing a predictive tool that helps operators optimize cleaning strategies without compromising filter performance. By accurately forecasting DO levels during and after UWS under various operational scenarios, the model enables the adjustment of sweetening flows and flow reintroduction rates required to prevent anoxic conditions.

This approach not only enhances the efficiency and reliability of SSFs but also has potential applications in other filtration methods where biological activity is critical, such as rapid sand filters or adsorption beds with bioactive layers. Globally, the model can assist water treatment facilities in improving operational protocols, reducing downtime, and maintaining high water quality standards, thereby contributing to better water quality management. This study introduces a refined model for predicting DO dynamics in SSFs with high accuracy, enhancing operational strategies for water treatment. The development and validation of this model advance UWS techniques, potentially improving global water quality management by enhancing water treatment strategies through other forms of filtration.

5. Conclusions

A mass balance model has been developed utilizing empirically derived DO consumption rate data to predict the impact of UWS under a number of different sweetening flows. Overall, the study has demonstrated that UWS offers no risk to the operation of SSFs compared to traditional skimming methods. This research suggests that the inclusion of a 'sweetening flow' during UWS could considerably improve DO supply, reduce the emergence of anoxic conditions, and expedite filter recovery time.

Implementation of the findings translates to setting the level of flow pause and the rate of introduction as a function of temperature. Importantly, the results show that higher temperatures pose the most challenge due to the combined impact of reduced DO solubility and increased microbial activity. Accordingly, agreed practice should be based on summer conditions. The study also identifies the *Schmutzdecke* and GAC layers as the highest DO consumers that remain stable once the bed matures. More insight concerning the range of DO utilization rate observed in these layers in other SSFs is required to understand the calibration requirements for using this model on other sites and to what level standard numbers can be used.

Abbreviation

DO	dissolved oxygen
SSF	slow sand filter
UWS	underwater skimming
GAC	granular activated carbon
SOUR	specific oxygen uptake rate
HLR	hydraulic loading rate
BV	bed volume
RMSE	root mean square error
TOC	total organic carbon
NTU	nephelometric turbidity unit

PBS phosphate-buffered saline

CRediT authorship contribution statement

Tolulope Elemo: Writing – original draft, Methodology, Investigation, Formal analysis, Data curation. **Michael Chipps:** Writing – review & editing, Supervision, Project administration, Funding acquisition. **Nigel Graham:** Writing – review & editing, Validation, Supervision. **Andrew Turner:** Writing – review & editing, Funding acquisition. **Bruce Jefferson:** Writing – review & editing, Supervision, Methodology, Funding acquisition, Conceptualization. **Francis Hassard:** Writing – review & editing, Supervision, Resources, Project administration, Methodology, Funding acquisition, Conceptualization.

Declaration of competing interest

The authors declare that they have no known competing financial interests or personal relationships that could have appeared to influence the work reported in this paper.

Acknowledgements

The authors acknowledge the financial support of the Engineering and Physical Sciences Research Council (ESPRC), through the STREAM Industrial Doctorate Centre (EP/L015412/1), and financial support from Thames Water and Northumbrian Water Group. The authors also appreciate the support provided by Affinity Water. The authors are grateful to Dr. Jenny O'Reilly, Ian Doggett, and Dr. Richard Lake for their valuable contributions.

Appendix A. Supplementary data

Supplementary data to this article can be found online at https://doi.org/10.1016/j.scitotenv.2024.176730.

Data availability

link shared on data

References

van der Aa, L.T.J., Rietveld, L.C., van Dijk, J.C., 2011. Effects of ozonation and temperature on the biodegradation of natural organic matter in biological granular activated carbon filters. Drink. Water Eng. Sci. 4 (1), 25–35.

Abdiyev, K., Azat, S., Kuldeyev, E., Ybyraiymkul, D., Kabdrakhmanova, S., Berndtsson, R., Khalkhabai, B., Kabdrakhmanova, A., Sultakhan, S., 2023. Review of slow sand filtration for raw water treatment with potential application in less-developed countries. Water 15 (11), 2007.

Altman, D.G., Bland, J.M., 1983. Measurement in medicine: the analysis of method comparison studies. Statistician 32 (3), 307.

Bland, J.M., Altman, D.G., 1999. Measuring agreement in method comparison studies. Stat. Methods Med. Res. 8 (2), 135–160.

Burman, N.P., 1978. Slow sand filtration. H_2O 11 (16), 348.

Campos, L.C., Smith, S.R., Graham, N.J.D., 2006. Deterministic-based model of slow sand filtration. I: model development. J. Environ. Eng. 132 (8), 887–894.

Cullen, T.R., Letterman, R.D., 1985. The effect of slow sand filter maintenance on water quality. J. Am. Water Works Assoc. 77 (12), 48–55.

Eighmy, T.T., Collins, M.R., Malley, J.P., 1993. Biologically Enhanced Slow Sand Filtration for Removal of Natural Organic Matter. American Water Works Association, USA, Denver, Colorado.

Elliott, M.A., DiGiano, F.A., Sobsey, M.D., 2011. Virus attenuation by microbial mechanisms during the idle time of a household slow sand filter. Water Res. 45 (14), 4092–4102.

Ellis, K.V., 1985. Slow sand filtration. CRC Crit. Rev. Environ. Control. 15 (4), 315–354.

Hassard, F., Elemo, T., Chipps, M., Turner, A., Jefferson, B., Graham, N., 2022. Underwater remote skimming of slow sand filters for sustainable water production. ACS ES&T Water 2 (9), 1471–1474.

van der Kooij, D., Veenendaal, H.R., van der Mark, E.J., Dignum, M., 2017. Assessment of the microbial growth potential of slow sand filtrate with the biomass production potential test in comparison with the assimilable organic carbon method. Water Res. 125, 270–279.

Langenbach, K., Kuschk, P., Horn, H., Kästner, M., 2010. Modeling of slow sand filtration for disinfection of secondary clarifier effluent. Water Res. 44 (1), 159–166.

Maiyo, J.K., Dasika, S., Jafvert, C.T., 2023. Slow sand filters for the 21st century: a review. Int. J. Environ. Res. Public Health 20 (2), 1019.

Schijven, J.F., Van den Berg, H.H.J.L., Colin, M., Dullemont, Y., Hijnen, W.A.M., Magic-Knezev, A., Oorthuizen, W.A., Wubbels, G., 2013. A mathematical model for removal of human pathogenic viruses and bacteria by slow sand filtration under variable operational conditions. Water Res. 47 (7), 2592–2602.

Steele, M.E.J., Evans, H.L., Stephens, J., Rachwal, A.J., Clarke, B.A., 2006. Dissolved oxygen issues with granular activated carbon sandwich slow sand filters. In: Gimbel, R., Graham, N.J.D., Collins, M.R. (Eds.), Recent Progress in Slow Sand and Alternative Biofiltration Processes. IWA Publishing, London, pp. 83–94.

Trikannad, S.A., van Halem, D., Foppen, J.W., van der Hoek, J.P., 2023. The contribution of deeper layers in slow sand filters to pathogens removal. Water Res. 237 (April), 119994.

US EPA, 2001. Method 1684: Total, Fixed, and Volatile Solids in Water, Solid, and Biosolids.

Velten, S., Boller, M., Köster, O., Helbing, J., Weilenmann, H.U., Hammes, F., 2011. Development of biomass in a drinking water granular active carbon (GAC) filter. Water Res. 45 (19), 6347–6354.

Wang, J.Z., Summers, R.S., Miltner, R.J., 1995. Biofiltration performance: part 1, relationship to biomass. J. Am. Water Works Assoc. 87 (12), 55–63.

Young-Rojanschi, C., Madramootoo, C., 2014. Intermittent versus continuous operation of biosand filters. Water Res. 49 (1), 1–10.

https://dspace.org/

Predicting the impact of underwater skimming on dissolved oxygen consumption in slow sand filters for potable water treatment

Elemo, Tolulope; Chipps, Michael; Graham, Nigel; Turner, Andrew; Jefferson, Bruce ...

2024-12-01
Elsevier
https://doi.org/10.1016/j.scitotenv.2024.176730
Elemo T, Chipps M, Graham N, et al., (2024) Predicting the impact of underwater skimming on dissolved oxygen consumption in slow sand filters for potable water treatment. Science of The Total Environment, Volume 954, December 2024, Article number 176730

Downloaded from a DSpace repository. https://dspace.org/